JOURNAL OF AIRCRAFT
Vol. 47, No. 4, July–August 2010

Engineering Notes

Quick Access Recorder Data Analysis Software for Windshear and Turbulence Studies

H. Haverdings*
National Aerospace Laboratory/NLR, 1059 CM Amsterdam, The Netherlands
and
P. W. Chan†
Hong Kong Observatory, Kowloon, Hong Kong, People's Republic of China

DOI: 10.2514/1.46954

Nomenclature

A_y	=	lateral acceleration
a_0–a_3	=	calibration coefficients
m	=	aircraft mass
T_{wndw}	=	window time interval
V	=	inertial speed
V_a	=	airspeed
V_w	=	wind speed
x, y, z	=	position coordinates
Y	=	side/lateral force
α	=	angle of attack
β	=	sideslip angle
δ_F	=	flap angle
$\varepsilon^{1/3}$	=	eddy dissipation rate
λ	=	bias in accelerometer
$\tilde{\sigma}_w$	=	standard deviation in vertical wind
τ	=	time lag
χ	=	track angle
ω_1, ω_2	=	cutoff frequencies in the calculation of eddy dissipation rate

Subscripts

fin	=	tail fin
fus	=	fuselage
wndw	=	window

Superscripts

b	=	body
e	=	Earth

I. Introduction

DUE to terrain effect and land–sea interaction, landing and departing aircraft at Hong Kong International Airport (HKIA) could experience low-level windshear and turbulence (viz., occurring below 1600 ft). On average, 1 in 500 flights at HKIA reports encountering significant windshear (headwind/tailwind change of 15 kt or more) and 1 in 2,000 flights reports significant turbulence (moderate or severe). To capture the wind fluctuations, a suite of ground-based and remote-sensing meteorological instruments is operated by the Hong Kong Observatory (HKO), including conventional anemometers, weather buoys, radar wind profilers, a terminal Doppler weather radar and two light detection and ranging (LIDAR) systems. Based on the data collected by these instruments, a number of windshear detection algorithms have been developed by HKO and put into operational use at HKIA. Turbulence detection algorithms are under development as well.

In the development and verification of the preceding algorithms, pilot reports are normally used as sky truth. However, it is commonly accepted that the pilots' perception of windshear and turbulence is subjective, and there could be discrepancies among the reports themselves. To build up an objective database of windshear and turbulence cases, HKO has taken two steps: 1) to obtain quick access recorder (QAR) data routinely from local airlines, and 2) to arrange a collaborative study with an established aerospace laboratory for developing software to process the QAR data and obtain the required meteorological quantities [e.g., the three wind components, windshear hazard factor, and turbulence intensity metrics, such as turbulent kinetic energy (TKE) and eddy dissipation rate (EDR)]. Similar work was done in this area by Bach and Parks [1] and others (see [2–5]).

II. Basic Features of the Algorithm WINDSTURB

A. General

The aircraft types considered so far include A320, A330, B747, and B777. The parameters measured onboard the aircraft vary from type to type. Basically, the QAR data can be grouped into several categories; viz., inertial data [e.g., accelerations, groundspeed (GS)], attitude data (e.g., pitch, roll) and attitude rates (if available), aerodynamic data (e.g., calibrated airspeed, Mach number, etc.), etc. The data sampling rates vary for the different parameters and also depend on aircraft type. It is assumed that proper presampling filters have been applied before recording the data. The basis of all postprocessing and calculations is a fixed sampling rate of 4 Hz. For this purpose, data interpolation or reduction is required for various parameters.

B. Heart of the Algorithm

Detailed descriptions of the algorithm can be found in [6]. Basically, what is needed to determine the wind vector $\mathbf{V}_w$ is the inertial speed vector $\mathbf{V}$ and the aerodynamic speed vector $\mathbf{V}_a$. The wind vector is simply obtained from the difference:

$$\mathbf{V}_w = \mathbf{V} - \mathbf{V}_a \tag{1}$$

These vectors relate to one and the same reference frame. The reference frames involved are the Earth-referenced frame (x, y, z)= (north, east, and vertical) , the runway reference frame (same as Earth frame but with x along the runway centerline), and the body reference frame (with its origin in the aircraft's center of gravity), the x axis pointing along the fuselage toward the nose, the y axis pointing toward the starboard wing tip, and the vertical z axis following the right-hand rule (i.e., downward). A particular reference frame is indicated by superscripts b or e for the body or Earth frame, respectively.

One could obtain the wind from the wind data computed by the flight management system (FMS) (the vertical wind component is

Presented as Paper 2009-3871 at the 1st AIAA Atmospheric and Space Environments, San Antonio, TX, 22–25 June 2009; received 31 August 2009; revision received 20 May 2010; accepted for publication 14 May 2010.

*Anthony Fokkerweg 2.
†134A Nathan Road.

not computed), but this information was not always found reliable or accurate. Therefore, it is computed using Eq. (1). The first term (the inertial velocity vector **V**) in the Earth reference frame is

$$\mathbf{V}^{e} = \begin{bmatrix} \mathrm{GS}\cos\chi \\ \mathrm{GS}\sin\chi \\ \dot{z} \end{bmatrix}^{e} \tag{2}$$

The second term (the aerodynamic velocity vector) is obtained in the body reference frame as follows:

$$\mathbf{V}_{a}^{b} = \begin{bmatrix} V_a\cos\alpha\cos\beta \\ V_a\cos\alpha\sin\beta \\ V_a\sin\alpha \end{bmatrix}^{b} \tag{3}$$

Thus, one needs to know the aerodynamic speed V_a, the angle of attack (AOA) α, and the sideslip angle β. The aerodynamic speed is computed using a combination of calibrated airspeed, Mach number and/or true airspeed (if recorded on the QAR), etc. Sections II.D and II.E describe how α and β are obtained.

In subtracting the velocities in Eq. (1), these are referenced in the same reference frame, using suitable axis transformations.

C. Kalman Filtering and Smoothing

A main feature of WINDSTURB is the use of Kalman filtering and smoothing. It is a process of estimating the state vector **x** of a dynamical system at a particular stage i (or time t_i) and its covariance, where **x** consists of three inertial velocities, three positions, and three accelerometer biases, using measurements of inertial data (e.g., track, GS), attitudes, barometric and radio altitudes, etc. Furthermore, estimates of the accuracy with which parameters have been measured were derived, sometimes by trial and error. The Kalman filter process is generally well known in literature; however, the smoothing process has not found wide application. Both are described in detail in [7]. The Kalman filter–smoother combination was applied specifically in order to estimate the vertical velocity as accurately as possible.

A typical result is given in Fig. 1, which shows the estimate of the inertial vertical velocity $\dot{z}$, as well as its standard deviation $\sigma_{\dot{z}}$ as it developed for a particular landing approach.

The vertical velocity varies from +4 m/s (descent at 790 feet per minute) to near zero at $t = 250$ s and, finally, back to zero again at the end (landing). The standard deviation of the vertical velocity starts off at about 0.7 m/s, and then it drops quickly to 0.5 m/s, where it more or less stays constant (the steady-state value). At the point where the more accurate radio altitude is used (about 400 s), it drops further to 0.2 m/s. This shows that the overall accuracy in the estimated vertical velocity, and hence the wind component, is in the order of 0.5 m/s (1 kt) or better, but it also shows that it is a dynamic process.

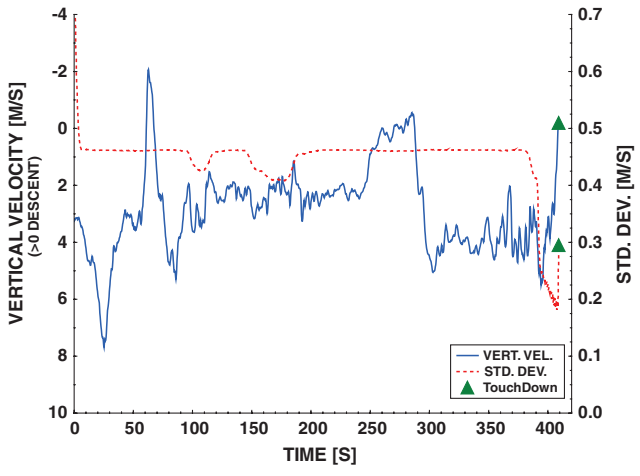

Fig. 1 Envelope of vertical velocity and standard deviation.

D. Angle-of-Attack Calibration

One aerodynamic parameter needed in Eq. (3) is the AOA α, to be obtained from the measured AOA vane data. The relationship between these two is the calibration equation. Since these calibration data are usually proprietary, they were derived from the QAR data.

Posing the calibration equation generally as

$$\alpha_i = a_o + a_1.\mathrm{AOA}_{i+\tau} + a_2.\delta_{F_i} + a_3.\mathrm{AOA}_{i+\tau}.\delta_{F_i} \tag{4}$$

the calibration coefficients a_0–a_3 and time delay τ are determined once per aircraft type through a multiple regression analysis.

E. Sideslip Angle Estimation

In all the QAR data considered so far, there is no measurement of the sideslip angle, as it is assumed to be negligible, so an estimation process has been developed [6,8]. Principally, β is derived from the assumption that the lateral force on the aircraft comes from 1) the tail fin due to the sideslip angle and 2) the fuselage contribution due to sideslip. The lateral specific force Y/m equals the lateral acceleration (minus bias correction), so one can write

$$\frac{Y}{m} \equiv A_y - \lambda_y = \frac{Y_{\mathrm{fin}} + Y_{\mathrm{fus}}}{m} \tag{5}$$

After some manipulation, one can derive (see [8])

$$\beta = -K_\beta m(A_y - \lambda_y) \tag{6}$$

where K_β is a complicated function specific for each aircraft type. A typical time history of the sideslip angle for a B777 landing approach is shown in Fig. 2.

Average sideslip varied between ±2–3°. At the end of the flight, the sideslip peaks to +11° as the plane is sideslipping to counteract the crosswind. If wind computations had been uncorrected for β, then the computed wind direction would have lined up with the runway track.

All of the preceding computations can be cast into a computational flowchart, found in Fig. 3.

F. Turbulent Kinetic Energy and Windshear

Finally, the wind components from Eq. (1) are in the E frame: $\mathbf{V}_w^e = \mathbf{V}^e - \mathbf{V}_a^e = \mathbf{V}^e - [\mathbf{T}_{be}]^T\mathbf{V}_a^b$, where $[\mathbf{T}_{be}]$ is the body-Earth transformation matrix or, in component form,

$$\begin{bmatrix} V_{w_x} \\ V_{w_y} \\ V_{w_z} \end{bmatrix} = \begin{bmatrix} \dot{x} \\ \dot{y} \\ \dot{z} \end{bmatrix} - [\mathbf{T}_{be}]^T \begin{bmatrix} V_a\cos\alpha\cos\beta \\ V_a\cos\alpha\sin\beta \\ V_a\sin\alpha \end{bmatrix}$$

With the wind vector known, the windshear parameter hazard F is calculated from

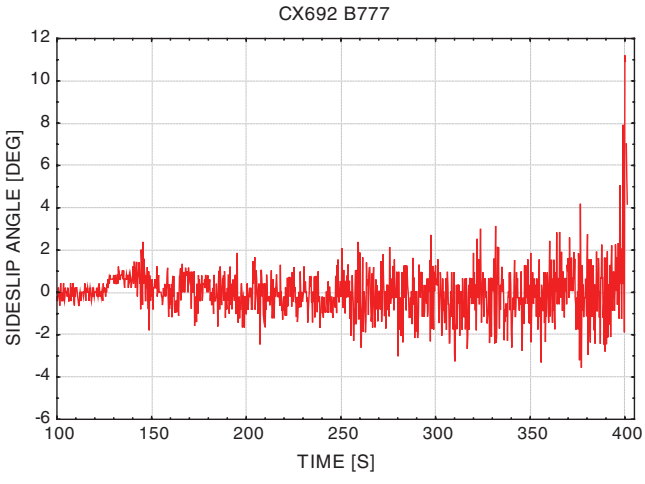

Fig. 2 Sideslip angle during typical flight (B777).

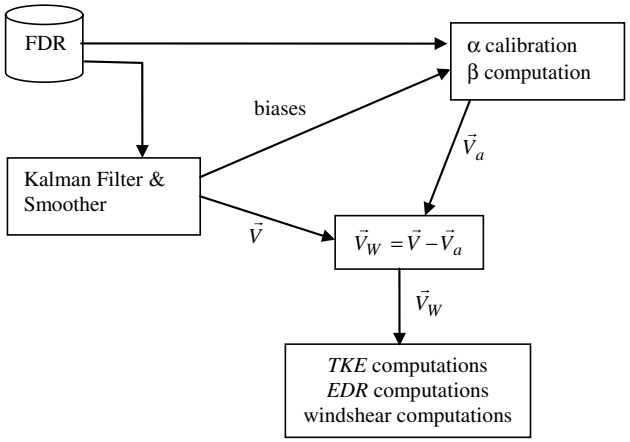

Fig. 3 Flowchart of relevant computations (FDR denotes flight data recorder).

$$F(t) = -\frac{1}{g}\dot{\mathbf{V}}_w(t) \cdot \frac{\mathbf{V}_a(t)}{\|\mathbf{V}_a(t)\|} - \frac{\mathbf{V}_w(t) \cdot \mathbf{k}}{V_a} \tag{7}$$

where **k** is the unit vector along the vertical axis (positive into the earth). The definition is such that, for a downdraft ($V_{w_z} > 0$), the F factor is negative, as an energy loss is implied.

The TKE is then computed from

$$\text{TKE} = \tfrac{1}{2}(\sigma_u^2 + \sigma_v^2 + \sigma_w^2) \tag{8}$$

The standard deviations σ_u, σ_v, and σ_w in the three wind components are computed around a central-moving average wind vector, with a window length of T_{wndw}, where T_{wndw} is specified by the program user.

III. Calculation of Eddy Dissipation Rate

The calculation of EDR requires the solution of the power spectrum of the vertical wind component over a selected time window. With the wind-based method preferred (see [9]), a more practical approach is to employ a running mean standard deviation calculation of the bandwidth-filtered vertical wind [10]:

$$\varepsilon^{1/3} = \frac{\widehat{\sigma}_w}{\sqrt{1.05 V_a^{2/3}(\omega_1^{-2/3} - \omega_2^{-2/3})}} \tag{9}$$

A sensitivity study of EDR computation with respect to the input parameters (see [10]) showed that there is no need to apply a low-pass filter to the vertical wind signal. Only high-pass filtering is required. The influence of the high-pass frequency on EDR appeared to be rather small. It is suggested to use $f_1 = 2\pi\omega_1 = 0.1 - 0.2$ Hz and $f_2 = 2$ Hz in Eq. (9). The moving time window length of 10–20 s also appears to be appropriate.

IV. Application Examples

The first case is a windshear event, analyzed in [11] (a B747-400 landing at HKIA on 29 March 2005). The pilot reported encountering windshear of +40 kt headwind gain during landing. From the wind speed computed from the QAR data, there is a wind change (increase) of ~12 m/s (24 kt) at about 2 n mile from touchdown (Fig. 4).

This wind change is less than the magnitude of windshear reported by the pilot. To reveal what happened, the airspeed and GS of the aircraft are plotted together in Fig. 5.

At 3 n mile from touchdown, both the airspeed and the GS are almost the same. Then the airspeed increases by about 20 m/s (40 kt). However, the also GS increases but by about 10 m/s (20 kt) only. It turned out that the aircraft was under the control of autopilot C in command mode, but the autothrottles had not been engaged, so the pilot who was flying must have manually controlled the speed with

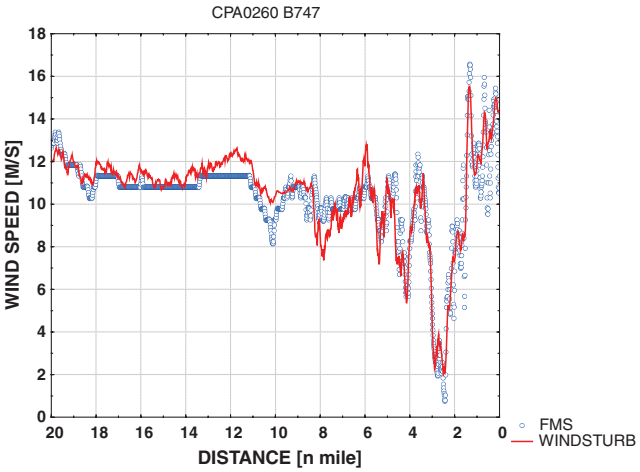

Fig. 4 Wind variation along the approach.

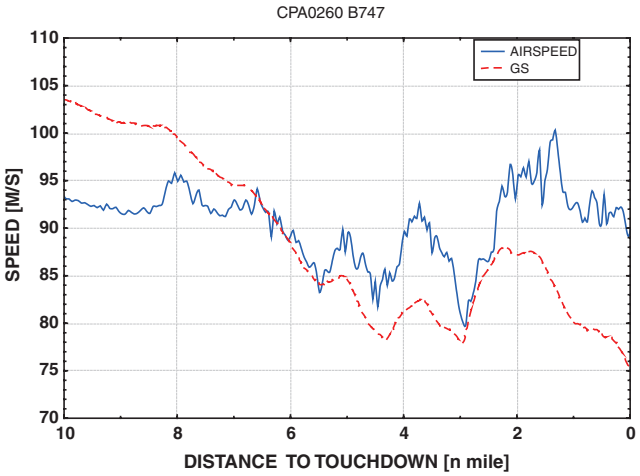

Fig. 5 Airspeed and GS versus distance to touchdown for the B747 flight.

the throttles. Therefore, the pilot-reported wind change of +40 kt was actually an airspeed change of +40 kt due to 1) a windshear of only 20 kt and 2) a GS increase of 20 kt because of pilot action.

A second case concerns the effect of sideslip on the computed TKE and EDR. The change in turbulence, brought about by including the sideslip, is shown in Fig. 6 for a B777 flight.

The TKE with sideslip reached peak values of about 5.5 m^2/s^2, which is 37% higher than the nonbeta peak value of 4 m^2/s^2. The EDR is hardly affected by the sideslip (see Fig. 7), where the peak value of 0.28 $m^{2/3} \cdot s^{-1}$ indicates light turbulence [11].

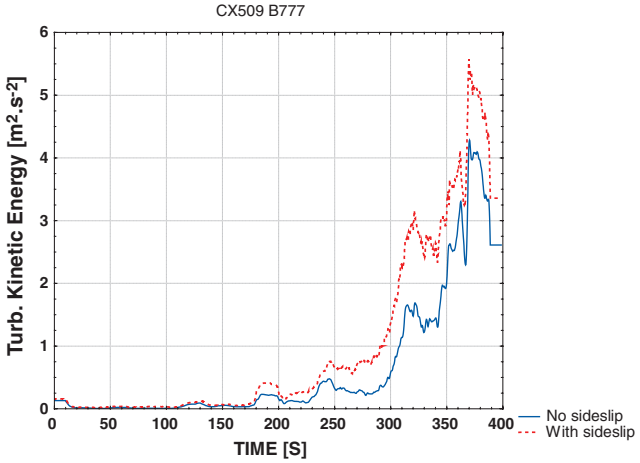

Fig. 6 Effect of sideslip gain on TKE.

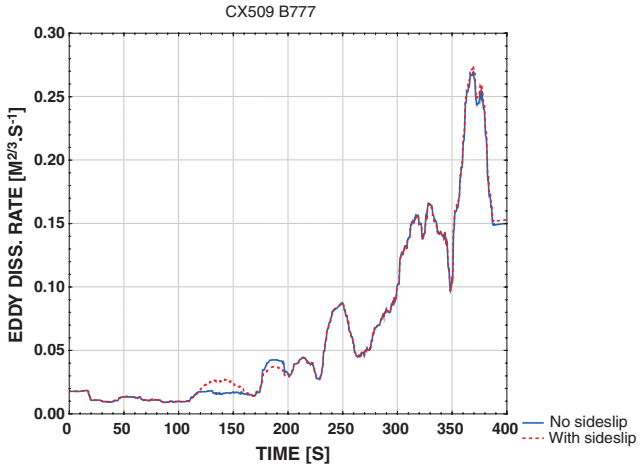

Fig. 7 Effect of sideslip gain on EDR.

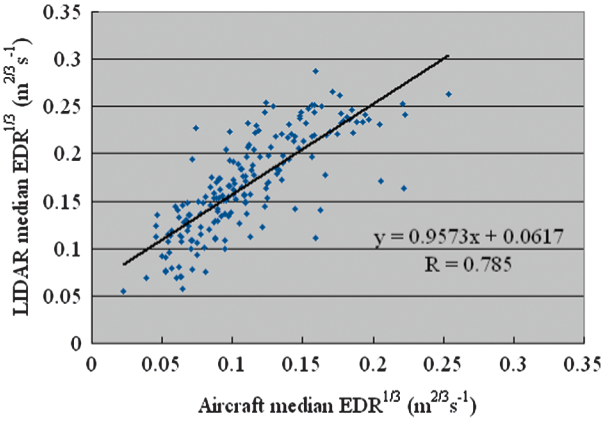

Fig. 8 Comparison of median $EDR^{1/3}$ values from the aircraft and from the LIDAR.

Finally, the computed EDR is compared against the LIDAR data measured at the airport [12] (see Fig. 8). Median $EDR^{1/3}$ values (between the runway threshold and 4 n mile away) are considered here. The comparison is based on 185 flights in 2006 and 2007. Technical details can be found in [12]. In general, the comparison between the two data sets shows a reasonable correlation.

V. Conclusions

A sophisticated algorithm has been developed by the National Aerospace Laboratory/NLR and HKO to calculate the meteorological parameters crucial for the study of low-level windshear and turbulence, using onboard QAR data. The resulting calculated windshear and turbulence parameters are found to give valuable insights into the low-level windshear and turbulence events at HKIA. The WINDSTURB program allows batch processing of large amounts of aircraft QAR data to be completed within several minutes.

The WINDSTURB software will be further refined to cover other aircraft types and expanded to handle missed approaches. The WINDSTURB-calculated F factor and EDR will also be compared more extensively with the estimates of these quantities from ground-based remote-sensing instruments and pilot reports.

Acknowledgment

The authors gratefully acknowledge the support of Cathay Pacific Airways, Ltd., which provided the quick access recorder data used in this study and the assistance of pilots for filing windshear reports to the Hong Kong Observatory for the purpose of enhancing flight safety.

References

[1] Bach, R. E., and Parks, E. K., "Angle-of-Attack Estimation for Analysis on Wind Shear Encounters," *Journal of Aircraft*, Vol. 24, No. 11, Nov. 1987, pp. 789–792. doi:10.2514/3.45522

[2] Bach, R. E., and Wingrove, R. C., "Analysis of Wind Shear from Airline Flight Data," *Journal of Aircraft*, Vol. 26, No. 2, Feb. 1989, pp. 103–109. doi:10.2514/3.45730

[3] Wingrove, R. C., Bach, R. E., and Schultz, T. A., "Analysis of Severe Atmospheric Turbulences from Airline Flight Records," *AGARD Flight Mechanics Panel Symposium*, AGARD, Neuilly sur Seine, France, May 1989; also NASA TM 102186, June 1989.

[4] Wingrove, R. C., and Bach, R. E., "Severe Turbulence and Maneuvering from Airline Flight Records," *Journal of Aircraft*, Vol. 31, No. 4, July–Aug. 1994, pp. 753–760. doi:10.2514/3.46557

[5] Cornman, L. B., Morse, C. S., and Cunning, G., "Real-Time Estimation of Atmospheric Turbulence Severity from In Situ Aircraft Measurement," *Journal of Aircraft*, Vol. 32, No. 1, Jan.–Feb. 1995, pp. 171–177. doi:10.2514/3.46697

[6] Haverdings, H., "Updated Specification of the WINDGRAD Algorithm," National Aerospace Laboratory/NLR TR 2000-623, Amsterdam, 2000, p. 68.

[7] Bryson, A. E., Jr., and Ho, Y. C., *Applied Optimal Control. Optimization, Estimation and Control*, Ginn and Co., Waltham, MA, 1969.

[8] Haverdings, H., "Improved Sideslip Estimation for Application to FDR Data Delivered by the Hong Kong Observatory," National Aerospace Laboratory/NLR CR 2008-223, Amsterdam, 2008, p. 40.

[9] de Bruin, A. C., and Haverdings, H., "Proposal for a Method to Compute Eddy Dissipation Rate from Flight Data Recorder Data," National Aerospace Laboratory/NLR CR 2007-137, Amsterdam, 2007, p. 29.

[10] de Bruin, A. C., and Haverdings, H., "Validation of an Eddy Dissipation Rate Calculation Method, Based on Flight Data Recording Data," National Aerospace Laboratory/NLR CR 2007-540, Amsterdam, 2007, p. 92.

[11] Haverdings, H., "FDR Analysis of 3 Cases Delivered by Hong Kong Observatory," National Aerospace Laboratory/NLR CR 2006-114, Amsterdam, 2006, p. 49.

[12] Chan, P. W., and Li, C. M., "Comparison of Turbulence Intensity Computed from LIDAR and Aircraft Data," *24th International Laser Radar Conference*, Boulder, CO, 23–27 June 2008.